Journal of Theoretical Biology 263 (2010) 530–543

Contents lists available at ScienceDirect

Journal of Theoretical Biology

journal homepage: www.elsevier.com/locate/yjtbi

ODE models for oncolytic virus dynamics ☆

Natalia L. Komarova [a,*], Dominik Wodarz [b]

[a] Department of Mathematics, 340 Rowland Hall, University of California, Irvine, CA 92697, USA
[b] Department of Ecology and Evolutionary Biology, 5205 McGaugh Hall, University of California, Irvine, CA 92697, USA

ARTICLE INFO

Article history:
Received 31 July 2009
Received in revised form
19 November 2009
Accepted 11 January 2010
Available online 18 January 2010

Keywords:
Oncolytic virus
Mathematical modeling
Differential equations
Cancer therapy

ABSTRACT

Replicating oncolytic viruses are able to infect and lyse cancer cells and spread through the tumor, while leaving normal cells largely unharmed. This makes them potentially useful in cancer therapy, and a variety of viruses have shown promising results in clinical trials. Nevertheless, consistent success remains elusive and the correlates of success have been the subject of investigation, both from an experimental and a mathematical point of view. Mathematical modeling of oncolytic virus therapy is often limited by the fact that the predicted dynamics depend strongly on particular mathematical terms in the model, the nature of which remains uncertain. We aim to address this issue in the context of ODE modeling, by formulating a general computational framework that is independent of particular mathematical expressions. By analyzing this framework, we find some new insights into the conditions for successful virus therapy. We find that depending on our assumptions about the virus spread, there can be two distinct types of dynamics. In models of the first type (the "fast spread" models), we predict that the viruses can eliminate the tumor if the viral replication rate is sufficiently high. The second type of models is characterized by a suboptimal spread (the "slow spread" models). For such models, the simulated treatment may fail, even for very high viral replication rates. Our methodology can be used to study the dynamics of many biological systems, and thus has implications beyond the study of virus therapy of cancers.

1. Introduction

Cancer therapy by means of oncolytic viruses has attracted attention of clinicians, wet lab oncologists and mathematical modelers (Bell, 2007; Bell et al., 2003; Crompton and Kirn, 2007; Davis and Fang, 2005; Kaplan, 2005; Kelly and Russell, 2007; Kirn and McCormick, 1996; McCormick, 2003, 2005; Novozhilov et al., 2006; O'Shea, 2005; Parato et al., 2005; Post et al., 2005; Roberts et al., 2006; Vaha-Koskela et al., 2007; Wodarz, 2001, 2003). The idea behind this treatment is to infect a tumor with engineered viruses which specifically infect and kill tumor cells, and have the potential to spread throughout the tumor. Healthy cells are largely spared. The aim is that the virus drives the tumor extinct and then goes extinct itself. Examples of such viruses include adenoviruses (such as ONYX-015), vesicular stomatitis virus (VSV), Newcastle disease virus (NDV), and several others.

While some encouraging results have been published in clinical trials (Aghi and Martuza, 2005; Davis and Fang, 2005; Lorence et al., 2003; McCormick, 2005), systematic and reliable tumor eradication by oncolytic viruses has not been achieved. Computational methods, including mathematical modeling, have been suggested as one of the tools to untangle the problem and achieve a better understanding of cancer-virus dynamics, with a goal of designing better treatment strategies (Bajzer et al., 2008; Dingli et al., 2006; Friedman et al., 2006; Novozhilov et al., 2006; Wein et al., 2003; Wodarz, 2001; Wodarz and Komarova, 2005). Such studies have lead to some useful insights, but a common feature of these approaches is that they contain arbitrary mathematical expressions to describe biological processes of uncertain nature. An important example are ODE models of virus dynamics, and in particular, the expressions that are used to describe the infection of cells. These are typically mass action terms in which the viral infectivity is simply proportional to the number of uninfected and infected cells. This tends to lead to "boom and bust" dynamics in which unrealistically strong oscillations are observed in the population of viruses and cancer cells. The infection term can be altered in many ways to include saturation effects which are more realistic. However, the resulting dynamics strongly depend on the exact mathematical expressions that are used to describe this. These expressions in turn are arbitrary and their biologically correct form is not known.

In this paper, we construct a mathematical framework that is based on ordinary differential equations and that aims to reduce

☆ Funded by: NIH.
* Corresponding author. Tel.: +1 949 824 1268.
E-mail address: komarova@uci.edu (N.L. Komarova).

0022-5193/$ - see front matter © 2010 Elsevier Ltd. All rights reserved.
doi:10.1016/j.jtbi.2010.01.009

the arbitrariness of mathematical choices. We adopt a modeling approach whereby we list all the relevant biological facts that are known about various terms and try to perform a general analysis of the resulting system. In this way, all the results are a consequence of the explicitly stated biological assumptions, and not artifacts of arbitrary mathematical formulations. This methodology continues a long tradition of mathematical modeling in biology which goes back to Gauss and Kolmogorov, see e.g. (Sigmund, 2007). Our generalized analysis will provide a framework upon which to base model selection and validation procedures when applied to specific experimental data.

Apart from this, our analysis also provides new insights into the correlates of successful oncolytic virus therapy. We find that the behavior can be classified into two general groups, depending on the general characteristics of the infection term used. In one scenario, which we call the "fast-spread virus model", most infected cells will be able to contribute to virus spread. In this setting, there exists a clear viral replication rate threshold beyond which the virus is predicted to control or eliminate the cancer. In the second scenario, called the "slow-spread model", it is assumed that only some of the infected cells can contribute to virus spread, and the fraction of cells contributing to virus spread declines as the number of infected cells increases. In this case, there is no clear viral replication rate threshold beyond which virus-mediated tumor control or elimination is possible. Uncontrolled cancer growth always remains a possible outcome, especially if the initial number of cancer cells upon start of treatment is relatively high.

The rest of the paper is organized as follows. In Section 2 we describe the model construction. In Section 3 we define the two models of viral spread. In Section 4 we present the most general analysis of the system and explain how treatment outcomes depend on the viral replication rate for different types of viral growth. Section 5 contains case studies of fast and slow types of viral propagation. Section 6 is reserved for discussion and conclusions.

2. Model construction

Since arguably no fundamental laws can assist us in formulating a mathematical description of a biological cancer-virus system, empirical modeling has been used to gain insights about both the long-term treatment outcome and temporal dynamics of the treatment process. And as always with such studies, the major drawback is a certain arbitrariness of mathematical choices made by authors when designing their studies. While "simplicity" is often cited as a factor dictating the form of the empirical relations, a particular choice must always be checked for robustness. The outcome of a model should be compared with the outcomes of alternative models; it can be considered robust if it remains unchanged while different modeling choices are used which are still compatible with known biological constraints. If the outcomes change depending on the particular choice of (unknown) terms in the mathematical model, this may mean that the result is an artifact of the particular mathematical system used, and its meaning should be questioned. In this paper we aim to demonstrate how various choices of a modeler can affect model results.

We will restrict ourselves to the methodology of ordinary differential equations. This means that we will not be explicitly including spatial and non-local effects in our description; also, we will ignore all stochastic effects. Despite these well-known shortcomings, we believe that it is important to understand the consequences of ODE modeling before extending the framework to spatial and stochastic systems. Modeling features that are not robust under small changes of assumptions in the ODE systems are likely to remain non-robust in more complicated scenarios.

The basis of our model for the cancer-virus system is the interaction between the population of infected and uninfected cells (Nowak and May, 2000; Wodarz and Komarova, 2005). Two of the uncertain components of the model are (i) the cancer growth term and (ii) the infection term. We leave these as general functions of the two components of the population and explore the consequences of various biological assumptions. We will consider the dynamics of the cancer-virus system by looking at the numbers of infected (y) and uninfected (x) cells. We will adopt the following very general predator–prey type system:

$$\dot{x} = xF(x,y) - \beta y G(x,y), \tag{1}$$

$$\dot{y} = \beta y G(x,y) - ay. \tag{2}$$

Here, the function F reflects cancer growth and death processes, G is the rate of infection. The coefficient β in front of the infection term represents the viral replication rate. The virus-infected cells death rate is assumed constant and denoted by a. The particular form of the terms F and G is unknown, but there are several biologically motivated requirements that these function must satisfy. These requirements are listed below. One of the goals of the paper is to understand the consequences of these assumptions and investigate what kinds of dynamics they are compatible with.

Ultimately, we are interested in the conditions under which the virus can drive the tumor cell population extinct. Because we are dealing with ODEs describing population averages, extinction as such cannot occur in the equations. However, if the number of tumor cells drops below a threshold level (e.g. less than one cell remains on average), then we can consider treatment a success.

We do not include a separate equation for the free virus in the system. The turnover of free virus is fast compared to that of infected cells, allowing us to make a quasi-steady-state assumption. Also, we do not consider the effects of the immune system. While immunity is likely to play a role in the dynamics of oncolytic viruses in vivo, inclusion of immunity adds another layer of complexity and introduces a variety of highly uncertain biological assumptions. Unless we have gained a sound understanding of the dynamics in the simpler setting, it will be impossible to assess the impact of immune responses in a realistic way. The models explored here can nevertheless be applied to experimental data that document oncolytic virus dynamics in vitro or in simple in vivo settings that do not involve immune responses, e.g. Harrison et al. (2001).

2.1. Cancer growth term

The function F, which we call the growth rate, reflects both the rates of cancer cell division and death. For example, if both divisions and death events happen exponentially, that is, proportionally to the total number of cells, then F is the difference between the constant division and death rates. We assume that the net cancer growth term ($xF(x,y)$) satisfies the following biological requirements:

1. The function F is non-negative and continuous for all $x, y \geq 0$.
2. A symmetry requirement: $F(x,y) = F(x+y)$: the growth is controlled by infected and uninfected cells equally.
3. At the beginning, the growth is exponential: $\lim_{z\to 0} F(z) = 1$. Note that this requirement fixes the scaling of the time-variable. In general, if the initial growth-rate $\lim_{z\to 0} F(z) = r$,

we scale time $t'=tr$, and also use $a'=a/r$ and $\beta'=\beta/r$. The primes are dropped for convenience.

4. The growth slows down as the number of cells increases: $dF(z)/dz \le 0$.

Some examples are:

- Exponential growth: $F=1$,
- Surface growth in 3D: $F=(\eta/(\eta+x+y))^{1/3}$ and in 2D: $F=(\eta/(\eta+x+y))^{1/2}$. These expressions are derived as follows. We assume that the increment in the number of uninfected cells is proportional to the number of uninfected cells in the tumor surface. This in turn is proportional to $x/(x+y)$ (the total fraction of uninfected cells) times $(x+y)^{2/3}$ (the surface area of a spherical the tumor in 3D, similarly in 2D). We obtain the expression $x/(x+y)^{1/3}$, which we replace with $x(\eta/(x+y+\eta))^{1/3}$ in order to allow for "volume growth" on scales $x+y \ll \eta$.
- Linear growth: $F=\eta/(\eta+x+y)$.
- Logistic growth: $F=1-(x+y)/W$.
- Gompertzian growth: $F=\log(W+\eta)/(x+y+\eta)(\log(W+\eta)/\eta)^{-1}$.

Different aspects of modeling tumor growth kinetics are discussed in Adam and Bellomo (1997).

In all cases except for the exponential growth, there is a parameter (denoted by η or W in the expressions above) which defines at what spatial scale the growth slows down and departs from exponential. The growth is unlimited unless there is a point $z_*=x_*+y_*$ such that $F(z_*)=0$. In the examples above, logistic growth and Gompertzian growths are bounded: we have $x_*+y_*=W$. We point out that the particular growth terms presented above are listed for the purposes of illustration, and our approach is not restricted to these functional forms. On the contrary, in the sections below we will develop a very general theory where the results will be based on the biological assumptions underlying the model rather than particular choices of mathematical expressions.

2.2. Virus spread term

We assume that the virus spread term ($\beta yG(x,y)$) satisfies the following biological requirements:

1. The function G is non-negative and continuous for all $x,y \ge 0$.
2. For small values of x and y, the growth should be exponential to reflect perfect mixing:
$$\lim_{x\to 0}\lim_{y\to 0} G(x,y)/x = \lim_{y\to 0}\lim_{x\to 0} G(x,y)/x = 1.$$
3. The growth term must monotonically increase with x and y:
$$\frac{\partial(yG(x,y))}{\partial x} \ge 0, \quad \frac{\partial(yG(x,y))}{\partial y} \ge 0.$$
4. The growth *rate*, $G(x,y)/x$, must slow down with x and y:
$$\frac{\partial(G(x,y)/x)}{\partial x} \le 0, \quad \frac{\partial(G(x,y)/x)}{\partial y} \le 0.$$
5. The growth has to be saturated in both x and y, such that
$$\lim_{x\to\infty} yG(x,y) = H_x(y), \quad 0 < H_x(y) < \infty,$$
where $H_x(y)$ is a function of y independent of x. Similarly, with y.
6. For large values of x, the growth term cannot be positive in the limit of small y, that is,
$$\lim_{y\to 0} H_x(y) = 0.$$
Similarly, with x.

Table 1
Some examples of virus spread terms.

$G(x,y)$	$H_x(y)$	$H_y(x)$	Fast or slow?
$x/(x+y+\varepsilon)$	y	x	Fast
$\frac{x}{\sqrt{x+y+\varepsilon_1}(\sqrt{x}+\sqrt{y}+\sqrt{\varepsilon_2})}$	y	x	Fast
$\frac{x}{(x+\varepsilon_1)(y+\varepsilon_2)}$	Const	Const	Slow
$\frac{x}{(\sqrt{xy}+\varepsilon_1)(\sqrt{x}+\sqrt{y}+\sqrt{\varepsilon_2})}$	$\sqrt{y}$	$\sqrt{x}$	Slow
$\frac{x}{\sqrt{x}(y+c)+x+\varepsilon}$	y	$\sqrt{x}$	Slow

7. For large values of x and y the spread cannot stop completely:
$$\lim_{x\to\infty}\lim_{y\to\infty} yG(x,y) = \lim_{y\to\infty}\lim_{x\to\infty} yG(x,y) > 0.$$
Note that this expression could be infinite.

Table 1 presents examples of virus spread terms allowed by above requirements. The meaning of the "fast" and "slow" is explained later in the paper. The different virus spread terms are based in part on the work done in the context of epidemiological models of infectious diseases, reviewed in McCallum et al. (2001). Note that the most frequently used infection term, $yG(x,y)=xy$, does not satisfy assumption 5 above. This term corresponds to complete mass-action, and can be viewed as $\lim_{\varepsilon\to 0}(1+\varepsilon)xy/(x+y+\varepsilon)$, see the first term in Table 1.

2.3. The scales of cancer growth and virus spread

Unless cells divide exponentially ($F=1$), there is at least one spacial scale defined by the function F which is related to the colony size at which the growth slows down and deviates from exponential. Let us denote the corresponding quantity s_t, where the subscript t stands for "tumor". The quantity s_t can be obtained from each particular function F. For example, in the case of linear growth, $s_t \sim \eta$. The units of the quantity s_t are the same as the units of x, which can be volume, mass of the number of cells. The (linear) spacial scale is thus related to $s_t^{1/3}$. Note that in the general case, the function F could have many parameters corresponding to different scales on which the growth law changes, but in many intuitive cases we envisage a growth which starts off as exponential and then deviates from it. Therefore, we can think of the quantity s_t as the colony size at which cancer growth first starts to slow down.

In a similar way we can define the value s_v, where v stands for "virus". This is defined as a characteristic size at which the infection spread become slower than exponential. To clarify this in the context of our system, let us consider the equation $\dot{y}=\beta xy-ay$ and assume that the pool of susceptible cells is large and constant. We can see that in this case the number of infected cells grows exponentially as long as $\beta x > a$. This may be a good approximation if the system size is small, but for larger values of x and y this cannot hold anymore. The scale at which the growth of infected cells deviates from exponential is s_v.

In what follows we will present a rigorous analysis of system behavior for different types of functions G and F. An intuitive understanding of these results can often be achieved by thinking about the two characteristic scales, s_t and s_v and how they trade off and influence the dynamics of disease spread and treatment.

3. Equilibrium solutions and two classes of virus spread

The fixed points of system (1)–(2) are given by $(0,0)$ and all the solutions to the equations

$$xF(x+y) = ay, \tag{3}$$

$$G(x,y) = \frac{a}{\beta}. \tag{4}$$

The trivial point $(0,0)$ has eigenvalues $F(0)$ and $-a$ and is thus a saddle. The number of solutions to Eqs. (3)–(4) depends on the particular shapes of the functions F and G. In order to find the non-trivial equilibria, we solve Eq. (3) to find $y(x)$, and then substitute it into Eq. (4). The equilibria are thus defined by the roots of equation

$$G(x, y(x)) = a/\beta. \tag{5}$$

The behavior of the function $G(x)$ is rigorously studied in Appendix A. In particular, we show that it is zero for $x=0$, and that as $x\to\infty$, the function $G(x)$ approaches a finite limiting value, which can be zero or non-zero.

Let us suppose that $F=1$, that is, the cancer cells grow exponentially. Solving Eq. (3), we obtain

$$y(x) = x/a \equiv y_{exp}(x),$$

the above expression defines the function $y_{exp}(x)$. Further we introduce the notation

$$G_{exp}(x) = G(x, y_{exp}(x)).$$

Depending on the behavior of the function $G_{exp}(x)$, we will separate all functions G into two classes in the following way. If

$$\lim_{x\to\infty} G_{exp}(x) = 0$$

then we will regard the virus spread to be *slow*. If

$$\lim_{x\to\infty} G_{exp}(x) = G^{\infty}_{exp} > 0,$$

with $G^{\infty}_{exp} < \infty$, we will regard this as *fast* spread. Examples of fast and slow virus spread terms are given in Table 1.[1] Note that we used the exponential cancer growth law, $F=1$, to define the two classes of G. It turns out that the definitions of slow and fast spread defined above are useful when studying any other cancer growth models. In the next sections we explore the mathematical consequences of the virus term being fast or slow, and show how changes in the cancer growth term affect the dynamics.

3.1. Fast virus spread

Fig. 1 presents a graphical way of solving Eq. (5) by plotting the left hand side and the (constant) right hand side as functions of x for different values of the parameter β. The number of intersections of $G_{exp}(x)$ with the constant function β/a equals the number of roots in Eq. (5).

In the case of fast virus spread, the function $G_{exp}(x)$ is either a monotonically increasing function (Fig. 1(a)), or it can attain one or more local extrema before converging to its non-zero horizontal asymptote, G^{∞}_{exp}, Fig. 1(b). In all cases, low values of β correspond to zero roots in Eq. (4), which means that the cancer growth will continue indefinitely. As β crosses a critical value, which we call β_c, one or more roots appear in Eq. (4), which signals a possibility of treatment success. The threshold values of β are shown on diagrams below each graph in Fig. 1.

[1] Note that the mass-action virus spread term, which corresponds to $G(x,y)=x$, can be classified as "super-fast", because in this case $G_{exp}(x)$ diverges as $x\to\infty$.

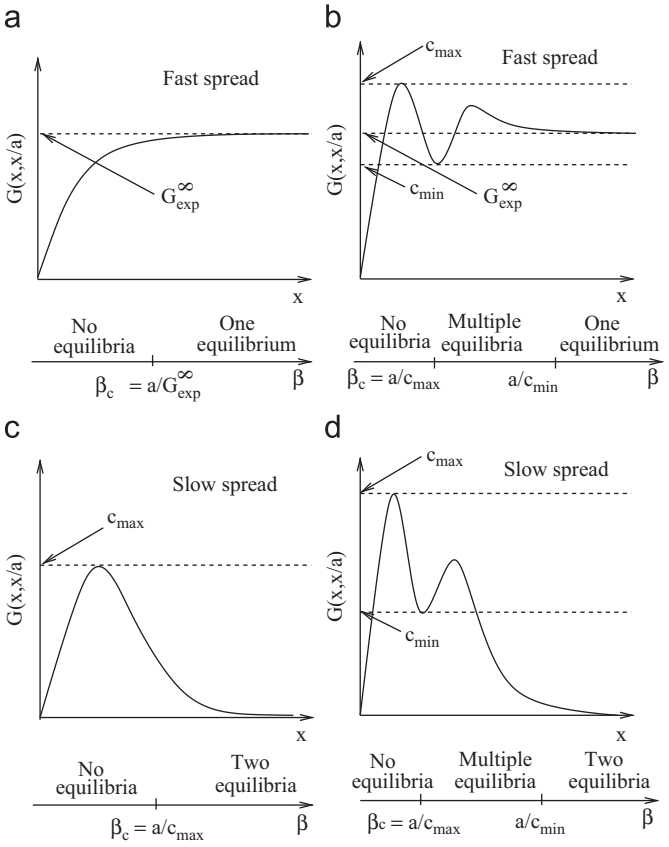

Fig. 1. The shape of the function $G_{exp}(x)$ and the number of equilibria as a function of β. (a,b) Fast virus spread. (c,d) Slow virus spread.

For a monotonically increasing G_{exp} (Fig. 1(a)), as β crosses a critical value defined by $\beta_c = a/G^{\infty}_{exp}$, exactly one root appears in Eq. (4). The value of x at this root drops as β increases (this is due to the convergence of G_{exp} to an asymptote, G^{∞}_{exp}). For large values of β, the value of x at the intersection tends to zero.

If the function G_{exp} attains one or more local extrema (Fig. 1(b)), we will refer to the lowest local minimum of the function $G_{exp}(x)$ as c_{min}, and to its highest local maximum as c_{max}. In this case, an initial increase of β above $\beta_c = a/c_{max}$ results in the appearance of two roots. Additional local extrema will result in appearance and disappearance of pairs of roots. However, as β increases through a second threshold, only one (the lowest) root remains. This second threshold is given by a/c_2, where c_2 is the lower of the values $\{G^{\infty}_{exp}, c_{min}\}$.

In all cases, for sufficiently large values of β, there will be only one root in Eq. (4). Introducing other cancer growth laws can increase the limiting value of G thus decreasing the value of β_c. In the case of a monotonically increasing G_{exp}, there will be no qualitative change. If G_{exp} is one- or multiple-humped, the hump(s) may disappear. Whether this qualitative change happens depends on the relative size of the two spacial scales involved. The first scale is defined by the location of the maxima of G_{exp} and is related to the virus spread scale, s_v. The second scale is given by the size, s_t, at which cancer growth law starts to deviate from exponential. Once $s_t \sim s_v$ (or it is smaller), the limiting value of G becomes sufficiently large such that the "hump" disappears.

Fig. 2 illustrates the case where the function G_{exp} is monotonically increasing. We use a particular law of virus spread coupled with three different laws of cancer growth: exponential, surface growth and linear growth, see the three solid lines in the figure. In all cases, the function is monotonically growing with a horizontal asymptote. The slower the cancer

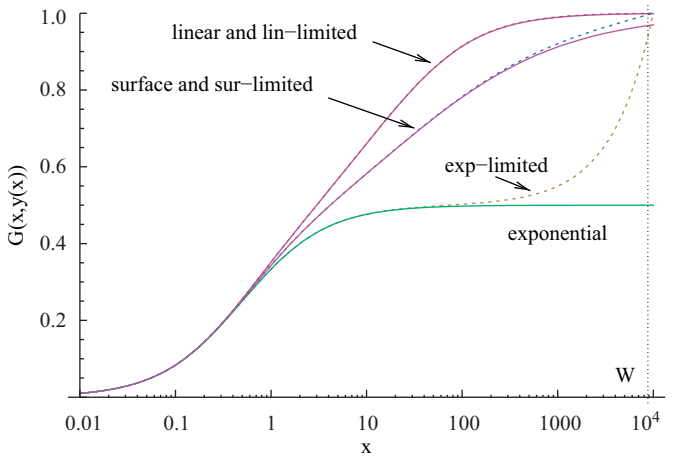

Fig. 2. Fast virus spread. The function $G(x,y(x))$ (Eqs. (3)–(4)) for the particular choice of the virus spread law ($G(x,y)=x/(x+y+1)$) and three different laws of cancer growth: exponential, surface growth and linear growth. The solid lines correspond to the unlimited cancer growth; the dotted lines—to a growth up to a given size, W. The parameters are: $a=1$, $\eta=10$ and $W=10^4$.

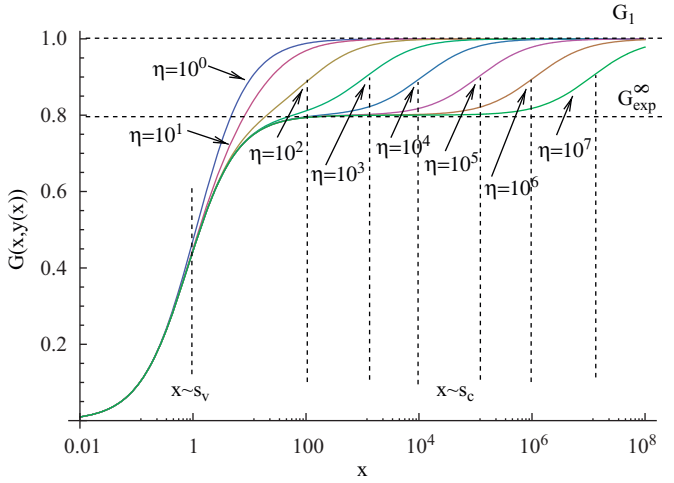

Fig. 3. The dependence of the equilibrium on β and s_t. We use the model with $F=\eta/(\eta+x+y)$ (thus, s_t is defined by η) and $G=x/(x+y+\varepsilon)$. The function $G(x,y(x))$ is plotted vs. x for different values of η. The dashed vertical lines indicate the scales of interest: the leftmost such line corresponds to $x\sim s_v$, and the rest of the lines to $x\sim s_t$ for different values of η. The other parameters are: $a=4$, $\varepsilon=1$.

growth, the higher is the asymptote and the lower is the threshold value, β_c, which corresponds to the possibility of treatment success.

It is useful to investigate the value of x at the equilibrium as a function of β, for different values of s_t. Suppose that the graph of $G(x,x/a)$ is a monotonically growing function of x which approaches a limiting value, G^∞_{exp}. Suppose that the cancer growth slows down around the scales near s_t. So near $x\sim s_t$, the function $G(x,y(x))$ deviates from the horizontal line G^∞_{exp}, and starts growing toward a different, and higher horizontal asymptote, which we will call $G_1>G^\infty_{exp}$, see Fig. 3 for a particular example. The phase diagram as β increases can be seen as follows: for $\beta<a/G_1$, there are no roots. As β crosses the first threshold, a/G_1, one root appears. The value of x at this equilibrium decays rapidly from infinity to values around s_t, as β grows (because of the fact that G_1 is a horizontal asymptote). Then as β grows through its second threshold, a/G^∞_{exp}, the value of x at equilibrium drops from s_t to values of order 1. The second transition is sharp if the following is satisfied: $s_t\gg x_1$, where x_1 is the value of x such that $|G(x_1,y(x_1))-G^\infty_{exp}|=|G_1-G^\infty_{exp}|$. In other words, x_1 is the value of x where the function $G(x,y(x))$ comes near the horizontal line defined by G^∞_{exp} ("near" means that it is at least as close to G^∞_{exp}, as G^∞_{exp} is to G_1). If $s_t\gg x_1$, then the function G has a significant interval in x where it approaches its horizontal asymptote, G^∞_{exp}, before it deviates from it to start growing toward G_1. This guarantees a threshold effect.

We conclude that for all cancer growth laws and for all functions G corresponding to fast virus spread, increasing β beyond a threshold leads to the existence of only one equilibrium, whose value correlates negatively with the infectivity, β. For large enough s_t, there is a "threshold" effect, such that the size at equilibrium decreases very sharply as β approaches a defined value. In biological terms, this class of models is always characterized by a viral replication rate threshold beyond which oncolytic virus therapy results in the elimination of the cancer.

3.2. Slow virus spread

In this case, the function $G_{exp}(x)$ is a one- or a multiple-humped function, which for large x decreases to zero (Fig. 1(c) and (d)). We refer to the global maximum of the function $G_{exp}(x)$ as c_{max}, and to the lowest local minimum (if it exists) as c_{min}.

In the case of an exponential growth, the bifurcation diagram looks as follows. As before, small values of β correspond to no equilibria (zero roots in Eq. (4)). As we increase β, a pair of roots appears after the threshold given by $\beta_c=a/c_{max}$. As β increases further, other roots may appear and disappear in pairs, see Fig. 1(d). Since the function G_{exp} has zero as its horizontal asymptote, there will be two equilibria for all values of β larger than a threshold. This threshold is given by a/c_{min}, if $G_{exp}(x)$ possesses a local minimum; it is equal to β_c otherwise. Two roots for large values of β is a universal feature of the systems with a slow virus spread term.

Let us next consider how non-exponential laws of cancer growth modify this picture. In the case of a linear growth, let us call the corresponding solution $y(x)$ of Eq. (3), $y(x)\equiv y_{lin}(x)$, and also $G_{lin}(x)\equiv G(x,y_{lin})$. The function $y_{lin}(x)$ converges to a non-zero constant, c_1, for large x, and we have $\lim_{x\to\infty}G_{lin}(x)=\lim_{x\to\infty}G(x,c_1)=G_x(c_1)=c_2<\infty$, which is a non-zero constant. Depending on the value of s_t, G_{lin} can take different shapes. For example, it can be a one- or a multiple-humped function. If s_t is similar or smaller than the location of the highest local maximum of G_{exp}, it will become a monotonically increasing function of x. In either of these cases, there exists a finite value of β given by a/c_2 such that for all values of β larger than this value, there is only one root in Eq. (4).

The following approximate estimate takes place. Let us suppose that the function $G_{exp}(x)$ has one local maximum. The position of the maximum is defined by the only spatial scale present in this case, which is s_v, that is, the scale on which the virus spread slows down. Therefore, roughly for $s_t\sim s_v$, treatment becomes possible. In other words, the cancer must slow down on spatial scales comparable or lower than the scale of virus spread in order to yield successful treatment.

By changing the function F, we make the cancer growth slower than exponential. In some cases (e.g. the case of linear growth described above), this will lead to the horizontal asymptote of $G(x,y(x))$ becoming non-zero. In general whether this happens depends on the functional forms of both G and F. For growths faster than linear but slower than exponential, we have $y\to\infty$ as x grows, but $y=o(x)$, i.e. it grows slower than x. In some cases the function G will retain a zero asymptote (e.g. in the case where

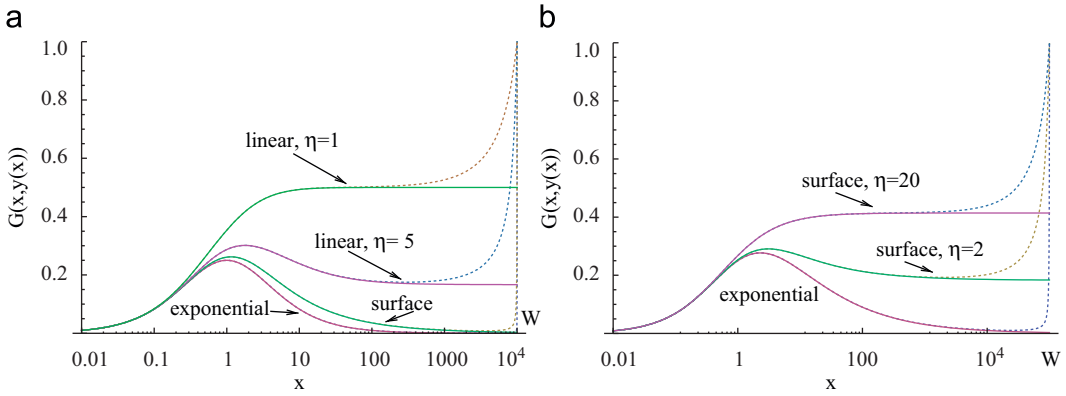

Fig. 4. Slow virus spread. The function $G(x,y(x))$ (Eqs. (3)–(4)) for two particular choices of the virus spread law: (a) $G(x,y)=x/(x+1)/(y+1)$ and (b) $G(x,y)=x/(x+1+\sqrt{x}(y+1))$. Different laws of cancer growth are implemented: exponential, surface growth and linear growth (in (a), with two values of η, $\eta=5$ and $\eta=1$). The solid lines correspond to the unlimited cancer growth; the dotted lines—to a growth up to a given size, W. The other parameters are: $a=1$, $W=10^4$ in (a) and $W=10^5$ in (b).

$G=x/(x+1)/(y+1)$ and a surface growth law for F). In other cases it will acquire a non-zero limit (e.g. with $G=x/(x+1+\sqrt{x}(y+1))$ and a surface growth law for F).

Two particular cases are illustrated in Fig. 4(a) and (b), solid lines. We can see that in (a), where we took $G=a/(x+1)/(y+1)$, both the exponential and surface cancer growth laws lead to a one-humped function G with a zero asymptote, which means that no matter how high β is, there are two roots in the system which corresponds to the existence of a saddle point and a possibility for the system to escape to infinity. A linear cancer growth leads to a one-humped function with a non-zero asymptote for larger value of s_t, and to a monotonically increasing function for smaller s_t, such that for β high enough, only one root exists which corresponds to cancer control.

Fig. 4(b) presents a different virus spread term, $G=x/(x+1+\sqrt{x}(y+1))$. We can see that for the surface growth, the particular function G presented in Fig. 4(b) acquires a non-zero limit. For this system, the growth of virus is slow (G_{exp} tends to zero), but if surface cancer growth is implemented, this results in a non-zero asymptote. In this case we can say that the surface cancer growth is sufficiently slow to warrant successful treatment given the particular mode of viral spread.

3.3. Bounded tumor growth

In all the considerations above we performed our analysis under the assumption of an unbounded cancer growth. Next, we consider a growth term which becomes zero in a finite time.

We assume that the growth starts off exponential ($F(0)=1$) and at some size, s_t, it slows down (we do not exclude the possibility that $s_t\sim 1$, that is, the growth becomes slower than exponential right away). Then there exists another characteristic size, $W\gg s_t$ such that the growth slows down further and stops. In particular, we define W such that $F(W)=0$. Note that if $s_t\sim W$ then there is no need to introduce the two scales, s_t and W. Therefore, the assumption $s_t\ll W$ must hold.

Now, we can see that the analysis above holds on the scales intermediate between s_t and W, such that $s_t\ll x\ll W$. In Figs. 2 and 4, the function G in the case of growth limited by a size W is plotted with dashed lines. For values $x\ll W$, the shape of the curve $G(x,y(x))$ is similar to that obtained for the corresponding unlimited growth. As x grows far beyond s_t and approaches W, the function G approaches $G(W,0)$. If, for the unbounded growth, the limiting value of the G function is c_2, we have in general $G(W,0)\geq c_2$. In other words, the curve G takes an upward turn in the vicinity of $x=W$. This means that Eq. (4) acquires an additional root corresponding to the cancer growing to its carrying capacity, W. In the systems with unrestricted growth this was equivalent to an unlimited growth of the cell population.

It is useful to note the following: in systems with a limited size, the function $G(x,y(x))$ is always bounded away from zero. Therefore, strictly speaking, we can always find a threshold value β_t such that for $\beta>\beta_t$, only one root is present. However, if $W\gg s_v$, such values of β are very large compared to β_c, and in most cases are probably not achievable.

4. Stability properties of the equilibria

Let us suppose that (x_0,y_0) with $x_0\geq 0$ and $y_0\geq 0$ is a solution to system (3)–(4), and consider its stability. The Jacobian of the system can be written as a 2×2 matrix,

$$J=\{m_{ij}\}=\begin{pmatrix} F+x_0F'-\beta y_0G_x & x_0F'-\beta(G+y_0G_y)\\ \beta y_0G_x & \beta y_0G_y\end{pmatrix},$$

where the functions F and G and their derivatives are evaluated at the point (x_0,y_0): $G_x=\partial G/\partial x|_{x=x_0,y=y_0}$, and similarly with G_y and F'. The equilibrium is stable if the following two conditions hold:

$$m_{11}+m_{22}<0, \tag{6}$$

$$m_{11}m_{22}-m_{21}m_{12}\geq 0, \tag{7}$$

where m_{ij} are components of the Jacobian matrix.

4.1. Saddle points

Condition (7) is equivalent to the positivity of the derivative of G in the direction defined by the implicit relation $ya=xF(x+y)$, Eq. (3). The latter expression is one of the two equations that define the equilibria. Differentiating it, we get: $ady=Fdx+xF'(dx+dy)$. The directional derivative is equal to $(G_xdx+G_ydy)=[G_x(a-F'x_0)+G_y(F+x_0F')]/(a-F'x_0)$. The denominator is positive, so this expression has the same sign as the left hand side of condition (7).

The equilibria are defined by the roots of Eq. (5). From Eq. (3) we can see that $y(0)=0$. We know from assumption (2) on the function G that $G(0,0)=0$. Therefore, all the odd roots of Eq. (5) will correspond to a positive, and the even ones to a negative slope of the left hand side of Eq. (5).

This means that all even equilibria are saddles. To prove this we note that in such cases, the directional derivative is negative, condition (7) is violated, and therefore there are two real

eigenvalues of opposite signs. On the other hand, an odd root can be either a sink, a source or a spiral (stable or unstable). This is because for such a root, condition (7) is always satisfied, so that we could either have complex eigenvalues, or real roots of the same sign (positive or negative).

In the presence of a saddle, an infinite outcome (corresponding to an unchecked cancer growth) is possible. For large values of x, we have

$$\dot{x} = xF^{\infty} - \beta y G^{\infty}(y), \tag{8}$$

$$\dot{y} = y(\beta G^{\infty}(y) - a), \tag{9}$$

where $\lim_{x\to\infty} G(x,y) = G^{\infty}(y)$ and $\lim_{x\to\infty} F(x,y) = F^{\infty}$. The growth of y becomes negative as y increases if $\lim_{y\to\infty} G^{\infty}(y) = 0$, which suggests that y settles to a finite value which make the right hand side of Eq. (9) zero, such that the outcome $(\infty, const)$ is observed. If $\lim_{y\to\infty} G^{\infty}(y) = const > 0$, then for large enough values of β we can have an outcome of the form (∞,∞).

4.2. Properties of the internal equilibrium

Let us first show that for large values of β, there will be an equilibrium, (x_0, y_0), such that $\lim_{\beta\to\infty} x_0 = 0$ and $\lim_{\beta\to\infty} y_0 = 0$. We call this equilibrium the "internal equilibrium". Its existence follows from Eq. (5) and the properties of the function G. We know that $y(0) = 0$, and also that $G(0,0) = 0$. It is also clear that there is an interval of x, $[0,\xi]$, where G is a growing function. Therefore, by continuity, for all $\beta \geq a/G(\xi, y(\xi))$, there will be a solution of Eq. (5). From monotonicity of the function G, the value of x at the intersection with a/β decays with β. From Eq. (3) it follows that there is an interval of x, $[0,\xi_1]$, where y is a growing function of x. Therefore, we conclude that for large enough β, there is an equilibrium, (x_0, y_0), whose values x_0 and y_0 decay with β and approach 0 in the limit $\beta\to\infty$.

Let us evaluate the left hand sides of inequality (6) for small values of x_0 and y_0. First, we approximate the curve $y(x)$ by its Taylor series for small values of x_0:

$$y_0 = Fx_0/a + (a+F)F'(x_0/a)^2 + (a+F)((F')^2 + 1/2(a+F)F'')(x_0/a)^3 + O[(x_0/a)^4], \tag{10}$$

where the function F and its derivatives are evaluated at 0. This expression follows from expanding both sides of Eq. (3) in Taylor series in terms of x_0 and y_0, solving for y_0 and using a Taylor expansion of this expression. Next, we express β from Eq. (4): $\beta = a/G(x_0, y_0)$. Now, let us multiply the left hand side of inequality (6) by $G(x_0, y_0)$, and use expression (10). Expanding in terms of small x_0, we obtain:

$$G(x_0,y_0)(m_{11}+m_{22}) = (F'G_x + G_{xy} - G_{xx}/2)x_0^2 + \frac{1}{a}\left((a+1)F''G_x + (a+2)F'G_{xy} + G_{xyy} + \frac{1}{2}((a-1)G_{xxy} - F'G_{xx}) - \frac{1}{3}aG_{xxx}\right)x_0^3 + O([x_0]^4). \tag{11}$$

Here the functions F and G and their derivatives[2] are evaluated at zero. To derive the above expression we also used the fact that the function G and its y-derivatives are equal to zero if $x = 0$, and $F(0) = 1$.

[2] Here we assume that the functions F and G are differentiable at zero. Non-differentiable functions are handled similarly by using generalized expansions.

Next, we evaluate the left hand side of inequality (7) in the same manner:

$$G(x_0,y_0)(m_{11}m_{22} - m_{21}m_{12}) = aG_x x_0 + (aF'G_x + 2G_{xy} + aG_{xx})x_0^2 + O([x_0]^3).$$

We can see that the expression above is always positive, so condition (7) is satisfied for large enough values of β. Condition (6) however is not necessarily satisfied, as follows from expression (11). The expansion can be positive or negative, depending on the particular properties of the functions F and G. Later we will encounter examples where the internal equilibrium changes stability depending on the model parameters.

Next, we would like to investigate whether the eigenvalues are real or complex. For the eigenvalues to have an imaginary part, the following condition has to be satisfied:

$$(m_{11} - m_{22}) + 4m_{12}m_{21} < 0. \tag{12}$$

Performing a Taylor expansion of the above expression for small values of x_0 and y_0 at internal equilibrium, we obtain

$$G(x_0,y_0)((m_{11}-m_{22}) + 4m_{12}m_{21}) = -4aG_x^2x_0^2 - 2G_x(2aF'G_x + 6G_{xy} + 3aG_{xx})x_0^3 + O([x_0]^4).$$

We can see that this quantity is always negative. Therefore, we conclude that the internal equilibrium has complex eigenvalues for sufficiently large values of β.

4.3. Is a fixed point analysis a valid tool?

Our investigations are primarily based on the analysis of fixed points of the cancer-virus system, and contain little information on the actual *dynamics* of the system's components. Therefore, one might argue that the picture provided by our analysis is incomplete. While this is a true statement, the fixed point analysis turns out to be sufficient to demonstrate the points we are making in this paper.

To illustrate this, let us first consider a system with a slow spreading virus. Our result is that there exists a saddle point which separates two possible equilibria, the larger one corresponding to treatment failure. We then conclude that the treatment outcome is uncertain in this situation because it depends on the initial conditions, even for very large values of viral infectivity, β. A fixed point analysis of this kind does not include the following scenario. The population could go extinct before it even had a chance to reach an equilibrium. However, in our case, such outcomes do not change the conclusions. The system *may* go extinct (which corresponds to treatment success), but it also *may not* which corresponds to treatment failure. The existence of a stable equilibrium corresponding to cancer growth means that even for very large values of the infectivity parameter, treatment failure may occur. Thus, even in the presence of dynamic extinction the outcome is "bistability", which is exactly the conclusion we reach.

Similarly, in the case of fast virus spread, our results remain unchanged by the process of dynamic extinction. For fast spreading viruses we show that for sufficiently large values of β, only one equilibrium is possible, which corresponds to very low cell numbers. We then conclude that this indicates a positive treatment prognosis. It is still possible that the system goes extinct before it reaches the "treatment" equilibrium, but in biological terms this corresponds to the same treatment outcome: cancer extinction.

5. Case studies of fast and slow virus spread models

In this section we will investigate properties of several fast-spread and slow-spread virus models and demonstrate how the dynamics change depending on the particular form of G.

5.1. Fast spread: equilibria and their stability

We start with the virus term defined by

$$G(x,y)=\frac{x(1+\varepsilon)}{x+y+\varepsilon}. \quad (13)$$

We refer to this term as "generalized frequency-dependent virus spread". Note that in the limit where $\varepsilon\to 0$ we have the conventional frequency-dependent spread term, $\beta xy/(x+y)$, and in the limit where $\varepsilon\to\infty$ we have βxy, the complete mixing approximation. Both are often used in SIR and predator–prey-type models (Anderson and May, 1991; McCallum et al., 2001).

Suppose that the cancer growth term is given (in dimensional variables) by $xrF(x+y)$. If we scale x and y in terms of ε, time in terms of r, and define $\beta'=\beta(1+\varepsilon)/(r\varepsilon)$ and $a'=a/r$, we get the following equations (omitting the primes):

$$\dot{x}=xF(x+y)-\frac{\beta xy}{x+y+1}, \quad (14)$$

$$\dot{y}=\frac{\beta xy}{x+y+1}-ay. \quad (15)$$

In steady state the following equations hold:

$$F(x+y)-\frac{\beta y}{x+y+1}=0, \quad (16)$$

$$\frac{\beta x}{x+y+1}-a=0. \quad (17)$$

Adding the two equations, and calling $z=x+y$, we obtain

$$\frac{\beta z}{1+z}=F(z)+a. \quad (18)$$

The left hand side of this equation is equal to zero at $z=0$, and it tends to β as z increases; this is a monotonically increasing function. The right hand side starts at $1+a$ for $z=0$, and it decays monotonically. For unlimited growth we have $\lim_{z\to\infty}F(z)=0$, and for limited growth $F(W)=0$, such that in both cases the right hand side tends to a for increasing x. Therefore, if $\beta>a$ for unlimited growth, or if $\beta>a(W+1)/W$ in the presence of a carrying capacity, W, then there is exactly one root in this equation. This root corresponds to a non-trivial amount of cancer and virus present. We will call the threshold value of β defined here β_c, and the corresponding equilibrium (x_0,y_0).

Other fixed points are $(0,0)$ (complete extinction) and $(W,0)$ (extinction of the virus) for growth with carrying capacity W; for an unlimited growth the latter fixed point is equivalent to growing off to $(\infty,0)$.

The point $(0,0)$ is unstable as long as $F(0)>0$ (non-trivial cancer growth from low numbers). The point $(W,0)$ is stable for $\beta<\beta_c$.

In Section 4.2 we showed that the internal equilibrium may or may not be stable depending on the model. Let us show that in the case of generalized frequency-dependent virus spread, the equilibrium (x_0,y_0) is stable as long as $\beta>\beta_c$. We perturb the system near the non-trivial equilibrium and write down the equation for the corresponding eigenvalues, Λ:

$$\Lambda^2x_0^2-\Lambda x_0F'(x_0+y_0)+aF^2(x_0+y_0)/(\beta y_0)-ay_0F'(x_0+y_0)=0. \quad (19)$$

Since $F'(x_0+y_0)\le 0$, the coefficient in front of Λ^0 is positive, which means that the two roots have the same sign. They are negative because the coefficient in front of Λ^1 is positive.

It turns out that for other parameterizations of G (which still correspond to fast virus spread) we may have an unstable equilibrium. Consider the following term G:

$$G=\frac{x}{\sqrt{x+y+\varepsilon_1}(\sqrt{x}+\sqrt{y}+\sqrt{\varepsilon_2})}. \quad (20)$$

By rescaling $x'=x/\varepsilon_2$ and $y'=y/\varepsilon_1$ and assuming for simplicity $\varepsilon_1=\varepsilon_2$, we obtain (in rescaled variables) the virus spread term $x/(\sqrt{x+y+1}(\sqrt{x}+\sqrt{y}+1))$. We will use the methodology of Section 4.2 to investigate the stability properties of the internal equilibrium for large values of β. An interesting feature of this dependency is that G is not differentiable in y at point $y=0$, and therefore expansion (11) cannot be used. Instead we need to use a generalized expansion of the left hand side in (6) to obtain

$$G(x_0,y_0)(m_{11}+m_{22})=\frac{1-\sqrt{a}}{2}x_0^{3/2}+\left(\sqrt{a}-\frac{1}{\sqrt{a}}+F'(0)\right)x_0^2+O([x_0]^{5/2}).$$

We can see that for $a>1$, the first term is negative, so that the equilibrium is stable. For $a<1$, it is unstable. For $a=1$, the first term is identically zero, and the second term is proportional to $F'(0)$, which is negative. We conclude that the equilibrium is stable for $a\ge 1$ and unstable otherwise.

It is interesting that the stability condition changes significantly if we modify the G term slightly. Let us use

$$G(x,y)=\frac{x}{\sqrt{x+y+1}(\sqrt{x+\delta_1}+\sqrt{y+\delta_2}+1)}.$$

Now, the function G is differentiable, and formula (11) can be used. We obtain the following expansion:

$$\left(\frac{\delta_1^{-1/2}+\delta_2^{-1/2}}{2(1+\sqrt{\delta_1}+\sqrt{\delta_2})^2}+\frac{F'(0)}{1+\sqrt{\delta_1}+\sqrt{\delta_2}}\right)x_0^2+O([x_0]^3).$$

Now the stability is defined by the values of $\delta_{1,2}$ and the derivative of F at zero.

Finally, we consider the example of the usual frequency dependent transmission, $G=x/(x+y)$ (see Eq. (13) with $\varepsilon=0$). This function has a singularity at 0. A generalized expansion yields for the left hand side of condition (6) (multiplied by $G(x_0,y_0)$):

$$\frac{aF'x_0}{1+a}+\frac{F''(1+a)-(F')^2}{1+a}x_0^2+O([x_0]^3).$$

This expression is negative for non-constant functions F, which means that the equilibrium is stable. For $F=1$ the real part of the eigenvalues is zero, which corresponds to neutral cycles in the dynamics.

Stability properties of the internal equilibrium for large values of the viral replication rate are defined by the behavior of the functions F and G at zero (for very small values of the populations x and y). By varying the functional form of G near zero we can in principle change the stability properties of the equilibrium. However this mathematical manipulation is not meaningful biologically. The difference between "stable" and "unstable" becomes apparent when the population diminishes to very low levels. The response of the system at the troughs of the oscillations is what makes them convergent or divergent. In biological terms, both outcomes probably correspond to extinction. Thus we conclude that for sufficiently large values of β, the cancer will be driven extinct by the virus through (convergent or divergent) oscillations.

5.2. Fast spread: the dependency of the equilibrium on β

As was shown in general terms in Section 3.1, the root of Eq. (18) is a monotonically decreasing function of β. Here we explore in some detail the threshold phenomenon in the context of some examples of fast virus spread terms. In particular, we would like to find the condition for the root to change in a threshold manner as a function of β. Suppose s_t is the size for which cancer growth deviates from exponential, and consider the roots of equation $G(x,y(x))=a/\beta$ for the generalized frequency-dependent virus spread G (Eq. (13)) and different types of F. For $x\ll s_t$, G comes close to the asymptote G_{exp} (which is given by $a/(a+1)$), see Fig. 3. For $x>s_t$, G tends to $\lim_{x\to\infty}G=1$. It is possible to show

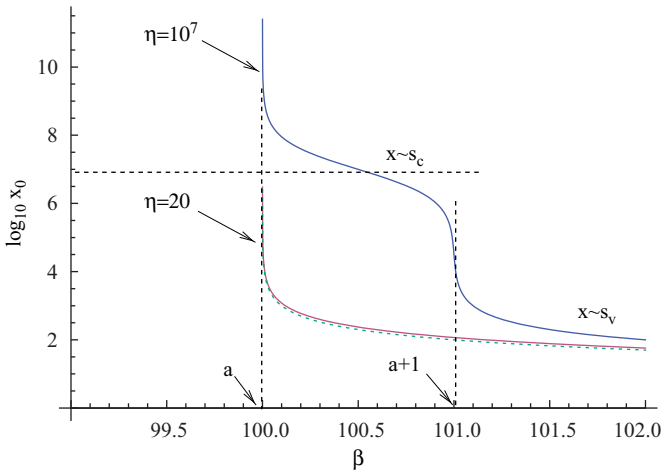

Fig. 5. The threshold-type dependence of the equilibrium number of cells on the infectivity. The steady-state value, x_0, is plotted as a function of β, for the model with $G=x/(x+y+\varepsilon)$ and $F=x/(x+y+\eta)$. The parameters are $a=10^2$, $\varepsilon=1$. The two solid curves correspond to the values $\eta=20$ and $\eta=10^7$. The dashed curve represents the approximation $x_0\approx a/(\beta\text{-}a)$.

that G is near $a/(a+1)$ when $x\sim a$ (we assume that $a\gg 1$ to derive that result). By "near" we mean that $G-a/(a+1)=a-a/(a+1)$, that is, the distance between the function G and its first asymptote[3] becomes smaller than the distance between the two asymptotes (and the latter could be small for large a). If $s_t\ll a$ then there is a large interval where G is close to its first asymptote before it deviates from it. Therefore, in such cases there is a very sharp decline of the equilibrium x value around the value $\beta=a+1$. Its value drops by the amount s_t-a while η increases from a to $a+1$. For an alternative explanation of the threshold behavior, see Appendix B.

The above analysis is illustrated in Fig. 5, where the equilibrium number of cells is plotted as a function of β for a particular choice of the function F (linear growth). We can see that for the upper curve corresponding to $s_t\gg a$ ($\eta\gg 10^7$), there are two threshold values of β. The first one is given by $\beta=a$. After this threshold a stable equilibrium appears whose value decreases from infinitely large values to values of the order of s_t (which is this model are given approximately by η). The second threshold value is given by $\beta=a+1$. As β crosses this value, the equilibrium rapidly decreases to values of the order s_v (given approximately by ε). The two threshold values are independent of the choice of F and are only defined by G.

While the presence of two threshold values of β is universal for all fast virus growths with large values of s_v, the actual threshold values are different for different systems. For example, for the term described in Eq. (20), the first asymptote has value $1-1/\sqrt{a}$ (for large values of a) while the second one is at 1. The value of x for which G becomes close to its first asymptote (in the sense described above) is given by $x\sim a^2$. Therefore, for values $s_t\gg a^2$, there is a sharp threshold in the behavior of the equilibrium near $\beta=a/(1-1/\sqrt{a})$.

In the opposite case where s_t is small, we can approximate $G(x,y(x))$ by $x/(x+1)$ and find that the value at the equilibrium is $x_0\approx\beta_c/(\beta-\beta_c)$, that is, there is no sharp transition in the dependency of the equilibrium on β for $\beta>\beta_c$. This can be seen in Fig. 5, where the lower solid curve corresponds to the plot of x_0 for $\eta=20<a$, and the dashed curve—to its approximation with $\beta_c/(\beta-\beta_c)$. Again, the particular dependency of the equilibrium value on β is not universal, for example, for G in Eq. (20), we have $x_0\propto(\beta-\beta_c)^{-2}$. The robust feature is that threshold behavior is not observed for small values of s_t. This makes sense from a biological point of view. If tumor growth saturates at relatively low levels, then treatment is easier. If the virus replicates fast enough to establish an infection in the tumor, it is likely to drive the tumor extinct. There is not a significant parameter region in which the tumor is maintained at relatively high level in the presence of the virus.

5.3. A particular slow virus spread model

In this section we concentrate on the following slow virus spread term:

$$G(x,y)=\frac{x(1+\varepsilon_1)(1+\varepsilon_2)}{(x+\varepsilon_1)(y+\varepsilon_2)}.$$

Let us keep the cancer growth term in its general form, F, and rescale the variables as follows: $x'=x/\varepsilon_1$, $y'=y/\varepsilon_2$, $t'=rt$, and define $\beta'=\beta(1+\varepsilon_1)(1+\varepsilon_2)/(r\varepsilon_1)$, $a'=a/r$ and $\lambda=\varepsilon_1/\varepsilon_2$. Omitting the primes, we obtain

$$\dot{x}=xF-\frac{\beta xy}{(x+1)(y+1)}, \tag{21}$$

$$\dot{y}=\frac{\beta\lambda xy}{(x+1)(y+1)}-ay. \tag{22}$$

As before, we assume that for all F except for the exponential, there is a parameter (denoted as s_t or W) which defines at what spatial scale the growth slows down and departs from exponential. The non-dimensionalized quantity measures the ratio of this spatial scale and ε_1.

As before, a convenient way to study the number of roots is to solve the equation $G(x,y(x))=a/(\beta\lambda)$, where $y(x)$ is obtained from

$$xF(x+y/\lambda)=ay.$$

For the exponential growth, $F=1$, $y\propto x$, and G is a one-humped function which decays to zero as $x\to\infty$. Therefore, as β increases, we acquire a pair of roots, which remain for all β. If the growth is superlinear, then $\lim_{x\to\infty}xF=\infty$, and therefore $\lim_{x\to\infty}y(x)=\infty$. Therefore, $\lim_{x\to\infty}G(x,y(x))=0$, and the behavior is qualitatively the same. Next, we consider linear growth. Now, $\lim_{x\to\infty}xF=c$, $0<c<\infty$, and thus $\lim_{x\to\infty}y(x)=c_1$ is also a non-zero constant (in our example with $F=\eta/(x+y+\eta)$, we have $c_1=\eta/a$). Therefore, $\lim_{x\to\infty}G=c_2$, a non-zero constant (for the particular law we consider here, we have $c_1=1/(\eta/a+1)$). If c_1 is sufficiently low, then we have two roots for an interval of β, and for larger values of β—only one root. However, if c_1 is large there may not be a second root. This happens if $s_t\sim s_v$ or $s_t<s_v$. In this case, as β crosses its critical value, only one root appears.

If the growth is limited, we have $F(W)=0$ for some $W=x^*+y^*$. Then $y(x^*)=0$, and $x^*=W$. We have $G(x^*,0)=x^*/(x^*+1)$ which is close to one for $W\gg 1$. The behavior of G near W introduces an additional root in the equation $G=a/(\beta\lambda)$; this root is located near $(W,0)$ and represents cancer grown to nearly its full capacity. This root is present as long as the saddle point is present, and it is always stable. Therefore, the behavior is as follows. For low values of β, the only stable root is the full cancer growth. Then, depending on the growth of cancer at intermediate scales (much smaller than W), either two additional roots appear, being a saddle, or the full growth root disappears and is replaced by an extinction root.

To summarize in biological terms, we recall that the virus spread is exponential before the mass reaches s_v (this is defined by constants $\varepsilon_{1,2}$); after that infection spreads much slower. If the tumor growth slows down/stops before the virus spread slows down, that is, if $s_t<s_v$, then the treatment is most likely to be successful, assuming

[3] The line G_{exp} is not an asymptote but rather a line that becomes an asymptote if $s_t\to\infty$.

that the infectivity, β, is sufficiently high. However, if the tumor growth is superlinear for sizes where the virus cannot spread fast anymore, i.e. if $s_t > s_v$, then treatment success is sensitive to the initial conditions, and only small tumors can be eradicated. The restriction on the initial tumor size becomes more stringent as the difference between s_t and s_v grows. If the virus spread slows down while the tumor still grows fast, and well before the tumor growth slows down, then treatment becomes nearly impossible.

In Appendix C we study three particular types of the cancer growth in the context of this slow virus spread model: exponential, logistic and linear growth. We discuss the equilibria, their stability, and the oscillatory behavior of the solutions.

6. Discussion and conclusions

This paper has provided a detailed mathematical analysis of an ODE modeling approach that investigates the dynamics of oncolytic viruses in a general setting, going beyond specific models in which results can depend on unknown and arbitrarily chosen mathematical formulations. This is very important if the aim is to generate predictive models, because the dynamics of the cancer and virus populations, and thus the correlates of successful therapy, can be heavily influenced by those unknown and arbitrary mathematical terms. We found that all possible 2-component ODE models can be divided into two categories with fundamentally different behaviors. We characterized those behaviors, and also investigated specific models that belong to the two different categories as case studies.

The main findings of this paper can be summarized as follows:

- All types of virus spread terms can be separated into two categories, which we call fast spread and slow spread.
- As expected, viral replication rate is an essential parameter which plays an important role in defining the treatment outcome. A less obvious factor which is just as important is the type of virus spread that is observed.
- For fast spreading viruses, there exists a viral replication rate threshold beyond which tumor control is the only outcome.
- For slow spreading viruses, we observe more complicated dynamics in which the outcome of therapy might go either way, depending on the initial number of cells and viruses.
- In systems with slow virus spread, we observe a race between the growth of the tumor and the spread of the virus. If the tumor growth slows down/stops before the virus spread slows down, then the treatment is most likely to be successful, assuming that the viral replication rate is sufficiently high. If the virus spread slows down while the tumor still grows fast, then treatment becomes nearly impossible even for very high viral replication rates.

Our results provide certain insights about the correlates of success in oncolytic virus treatment. Based on both previous experimental and theoretical work, it is believed that increasing the rate of virus replication will improve the chances of therapy success. In our terms, this notion is based on models where virus spread terms belong to the fast spreading class. In this paper we investigated different types of virus spread and demonstrated the existence of a second, slow class of virus spread. In this second class, successful therapy is more difficult to achieve, especially when tumor growth only saturates at larger tumor sizes. The outcome of the dynamics is predicted to depend on the initial conditions. If the number of cancer cells lies above a threshold, the cancer cell population will outrun the virus population, and therapy will fail. This creates problems because there is only a narrow window between the size at which the cancer is detected (about 10^{10} cells) and the size at which the cancer is lethal (about 10^{13} cells). In this case, increasing the rate of viral replication even to unrealistically large values will not significantly promote treatment success. Successful treatment is only possible if tumor growth saturates at relatively low tumor sizes. In this case, a parameter region exists in which tumor control is the only outcome. If tumor growth saturates at even lower sizes, this effect disappears altogether and tumor control is the only outcome. This suggests the strategy if combining oncolytic virus therapy with conventional treatment approaches which will limit tumor growth to a certain degree and allow the virus to gain the upper hand over the cancer. Previous data indicate that a combination of chemotherapy with virus therapy tends to be more effective than virus therapy alone.

In summary, studying constraints in the virus spread term, as well as the cancer growth term, has allowed us to gain new insights into the correlates of successful virus therapy. In particular, our results highlight potential difficulties in the treatment of tumors with virus therapy alone, even if the virus replicates with a relatively fast rate.

We would like to emphasize that our results pertain to the idealized situation of homogeneous tumors. It is a well-known fact that tumor therapy can fail due to the failure of the virus to penetrate and reach the core, e.g. because of intratumoral barriers or pressure. Such situations are not the focus of this paper; here we do not consider tumor inhomogeneities. Instead, we have found a much less obvious pattern. According to the model, for a virus spreading throughout a homogeneous solid tumor, it is still possible that the therapy fails, even for arbitrarily high virus infectivity parameters.

Next, we address the question of quantitative result interpretation and population extinction. It is a well-known fact that normally, ODEs cannot explicitly predict extinction (see also Novozhilov et al., 2006 for interesting results regarding this issue). Normally, size reduction to "low numbers" is interpreted as extinction, but then a question arises what numbers qualify as "low". Most of the graphs presented here are expressed in terms of rescaled variables. For example, x, the number of uninfected cells, is measured in the units of ε, the characteristic size of virus growth saturation. Therefore, "1" in the rescaled equations does not correspond to one cell remaining in the system. In order to relate the equations to observations, one needs to feed in the model parameters. For instance, once we have a measured value for the parameter ε, then we can rescale the variables back to their biological units and directly compare the growth/decay curve with "1". Values below 1 would signal extinction, and values much above 1 would mean survival of the colony.

The difficulty is of course in the parameter measuring. In our recent paper (Wodarz and Komarova, 2009) we performed data fitting of published data of oncolytic viruses, and concluded that even though many models can be found which are in a reasonably good agreement with the data, much more experimental information is needed in order to choose the "best" model. Future experimental studies will hopefully resolve the problem of model validation by (i) reducing the data spread by using larger samples, (ii) running the experiments for longer periods of time to obtain more points, and (iii) measuring some of the parameters directly. Once we know model parameters, the model can then be used for quantitative (and not just qualitative) predictions.

An advantage of our approach is its consistency and generality. A disadvantage is the fact that the less information we specify about the system, the less we can say about its behavior. For example, if we employ particular functional forms for functions F (the cancer growth term) and G (the virus spread term) and thus define the system of ODEs completely, then we can describe its behavior to any degree of precision, given the set of parameters and initial conditions. On the other hand, if only some (but not all) properties of the functions F and G are known, then the best we

can hope to achieve is to describe the phase space in some general terms. A very exciting result of this particular work is that despite a high degree of generality of the system, we were still able to generate a set of predictions about the system's behavior, both the dynamics and the long-term states.

We further note that the framework we used only contained two types of populations, uninfected and infected cancer cells. In reality other populations may play an important role in the dynamics, such as healthy cells, and the immune system. As mentioned before, it only makes sense to explore such added complexities once we have obtained a sound understanding of the basic dynamics between the virus and its target cells. Including the immune system will be a particular challenge for future mathematical work, since basic immune response dynamics can be described by a variety of mathematical functions that are unknown.

Our approach is necessarily limited by the choice of ODEs as our "toolbox". By restricting ourselves to this framework we make it impossible to take into account explicitly many essential properties of biological systems such as random fluctuations and spatial constraints. As mentioned before, some of the effects of spatial interactions are mimicked by the choice of rate terms F and G; however this is only a crude approximation whose validity is a topic of a separate investigation and is work in progress.

The other big topic is the inclusion of noise. In the present research we restricted ourselves to simply commenting that if the population of cells in ODEs drops to low levels, this probably means extinction in a stochastic system. Nonetheless we believe that the insights provided by our fully deterministic model are useful. The main theoretical result is that for "slow" virus growth, cancer control is not guaranteed even if the virus infectivity is arbitrarily high. On the other hand, if the virus spread is of the "fast" type, then the virus will control the tumor, given a high enough infectivity parameter. This result is independent of the stochastic modeling. That is, even though extinction described here will be mediated by stochastic fluctuations, the main driving force of extinction are dynamic interactions between cancer and virus. We do not need to explicitly include noise in the description in order to show the extinction. It is enough to show that in the deterministic model, the population will be driven to arbitrarily low levels (given that the infectivity is high enough and the virus spread is of the "fast" type). In our view, this proof of principle is a major result of the paper. We have found a pattern of behavior which is independent of details of modeling and particular assumptions. An extension of the present system to include stochastic effects is part of ongoing research.

The present paper is a conceptual basis for a more complex and biologically realistic modeling effort. We argue that this first step is necessary because complexity can only be explored layer by layer, with the more basic models being worked out first and the resulting insights used to shed light into the behavior of more realistic and relevant mathematical systems.

Acknowledgments

N.L.K. gratefully acknowledges the support of the Sloan Fellowship. D.W. and N.L.K. acknowledge the support of NIH Grant R01AI058153-01A2.

Appendix A. Supplementary calculations for the studies of the equilibria

In this section we study the properties of system (3)–(4). Non-trivial equilibria are obtained from Eq. (5). Let us consider the dependence of the left hand side of Eq. (5) on x. First, we study the behavior of $G(x,y(x))$ at $x=0$. Using Eq. (3), we obtain $y(0)=0$. From assumption 2 on the function G we obtain that $G(0,0)=0$, and from assumption 1 we see that this function grows for small values of x. Next, we study the limiting behavior of $G(x,y(x))$ for large values of x. For that we need to know the behavior of $y(x)$ for large x. We have from Eq. (3): $\lim_{x\to\infty} y(x)=\lim_{x\to\infty} xF(x)/a$. There are three cases:

(i) For a linear type growth, we have $\lim_{x\to\infty} xF(x)=c_0$, a non-zero constant. In this case, $\lim_{x\to\infty} y(x)=c_0/a$, with $0<c_0<\infty$.
(ii) For any growth F which is superlinear but slower than exponential, we have $\lim_{x\to\infty} y(x)=\infty$, but $\lim_{x\to\infty} y/x = \lim_{x\to\infty} F(x+y)/a=0$, that is, y increases slower than x.
(iii) Finally, for exponential growth, $F=1$ and $y(x)=x/a$, such that $y(x)\sim x$ for large values of x.

From the biological assumptions on the function $G(x,y)$ listed above, it follows that for any of the possible dependencies $y(x)$, the function $G(x,y(x))$ approaches a finite limiting value as $x\to\infty$, and this value can be zero or non-zero. To prove this statement we note that from requirement 5, $\lim_{x\to\infty} G(x,y)<\infty$ for constant values of y. For non-constant values of y we only need to show that the limit is finite in the case where $y\to\infty$. But from requirement 4 we deduce that if $\lim_{x\to\infty} y(x)=\infty$, then $\lim_{x\to\infty} G(x,y(x))\le\lim_{x\to\infty} G(x,const)<\infty$. This completes the proof.

The above statement is of course true for the function $G_{exp}(x)=G(x,y_{exp}(x))$. Note that for all laws of cancer growth slower than exponential, we have $G(x,y(x))\ge G_{exp}(x)$. This is because $y(x)\le y_{exp}(x)$, and G is a decreasing function of y.

Appendix B. Fast virus spread: threshold behavior and singular equilibria

In Section 5.2 for fast virus spread terms, we observe a sharp threshold behavior of the equilibrium as a function of the infectivity β for large values of s_t. This phenomenon can be explained in a different way. Let us consider the generalized frequency-dependent virus spread, and a particular realization of the term F, where cancer growth is supposed to follow a logistic curve, $F(x+y)=1-(x+y)/W$. In order to make some biological connections more transparent, we will not scale x and y with ε in this section, but rather work with the following system directly:

$$\dot{x}=x\left(1-\frac{x+y}{W}\right)-\frac{\beta(1+\varepsilon)xy}{\varepsilon+x+y}, \tag{23}$$

$$\dot{y}=\frac{\beta(1+\varepsilon)xy}{\varepsilon+x+y}-ay. \tag{24}$$

We will explore the behavior of this system in some detail, and in particular, consider the limiting case where $\varepsilon\to 0$. There are four fixed points in the system:

- $x=y=0$, complete extinction;
- $x=W$, $y=0$, extinction of the virus;
- $x=x_1>0$, $y=y_1>0$ (for $\varepsilon>0$), a fixed point corresponding to coexistence (non-trivial values) of both x and y;
- $x=x_2<0$, $y=y_2<0$ (for $\varepsilon>0$). The exact solutions for the latter two fixed points can be easily obtained; we do not present them here because they are rather cumbersome.

The first fixed point is unstable. The second fixed point is stable if the following condition holds:

$$\beta<\beta_c^1\equiv a\frac{1+\frac{\varepsilon}{W}}{1+\varepsilon},$$

where for small values of ε we have $\beta = a + O(\varepsilon)$. The third fixed point is stable as long as $\beta > \beta_c^1$, and the forth (negative) fixed point is always unstable.

The function $x_1(\beta)$ is a monotonically decreasing function of β. Let us consider the limit where $\varepsilon \to 0$. We define the second threshold value of β as $\beta_c^2 = a+1$, and study the asymptotic behavior of the fixed points for $\beta < \beta_c^2$ and $\beta > \beta_2^c$. Assume that the values of β are not too close to the second threshold, such that

$$|\beta - \beta_c^2| \gg \varepsilon.$$

Then we have the following expansions for the positive fixed point:

$$x_1 = \begin{cases} \dfrac{aW(a+1-\beta)}{\beta} + O(\varepsilon), & \beta_c^1 < \beta < \beta_c^2, \\ \dfrac{a\varepsilon}{\beta-(a+1)} + O(\varepsilon^2), & \beta > \beta_2^c, \end{cases}$$

$$y_1 = \begin{cases} \dfrac{(\beta-a)(a+1-\beta)}{\beta} + O(\varepsilon), & \beta_c^1 < \beta < \beta_c^2, \\ \dfrac{\varepsilon}{\beta-(a+1)} + O(\varepsilon^2), & \beta > \beta_2^c. \end{cases}$$

The negative fixed point satisfies

$$x_2 = \begin{cases} \dfrac{a\varepsilon}{\beta-(a+1)} + O(\varepsilon^2), & \beta_c^1 < \beta < \beta_c^2, \\ \dfrac{aW(a+1-\beta)}{\beta} + O(\varepsilon), & \beta > \beta_2^c, \end{cases}$$

$$y_2 = \begin{cases} \dfrac{\varepsilon}{\beta-(a+1)} + O(\varepsilon^2), & \beta_c^1 < \beta < \beta_c^2, \\ \dfrac{(\beta-a)(a+1-\beta)}{\beta} + O(\varepsilon), & \beta > \beta_2^c. \end{cases}$$

It is instructive to consider the behavior of the fixed points when $\varepsilon = 0$ (this limiting case was studied in detail by Novozhilov et al., 2006). We have two branches of solution for $\beta > \beta_c^1$. They correspond to

$$x \equiv \bar{x} = \frac{aW(a+1-\beta)}{\beta} \quad \text{and} \quad x = 0,$$

respectively, see Fig. 6, gray lines. The two branches cross over at point $\beta = \beta_c^2$. At this point we have a bifurcation, such that the solution $x = \bar{x}$ is stable for $\beta_c^1 < \beta < \beta_c^2$, and the solution $x = 0$ is stable for $\beta > \beta_c^2$ (stable solutions are represented by solid lines, and unstable ones by dashed lines). We can see that in this extreme case, for $\beta > \beta_c^2$, the system tends to extinction.

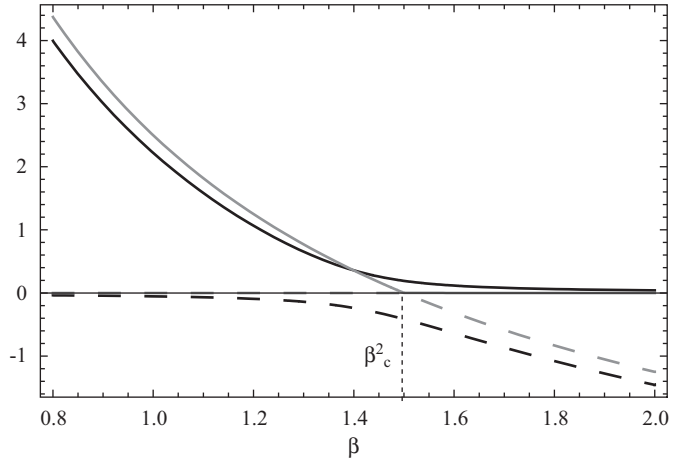

Fig. 6. Bifurcation diagram for the case $\varepsilon \ll 1$. The gray lines correspond to $\varepsilon = 0$ and the black lines to $\varepsilon = 0.05$. In the former case, the quantities $\bar{x}$ and 0 are plotted vs. β; in the latter case, the values x_1 and x_2 are plotted as functions of β. The solid lines represent stable solutions and dashed lines represent unstable solutions. The parameters are $a = 0.5$ and $w = 10$.

This bifurcation disappears as soon as $\varepsilon > 0$, see black lines in Fig. 6, but the qualitative interpretation of the solutions remains the same. For $\beta_c^1 < \beta < \beta_c^2$, we have a non-trivial coexistence equilibrium, and for $\beta > \beta_c^2$ the solution (which is still non-trivial) is vanishingly small, and it corresponds to extinction in a realistic generalization of our model where stochastic effects are included.

The fact that for $s_v = 0$, the branch $x = 0$ appears in the bifurcation diagram, is general and is independent of the exact form of the functions G and F. This can be seen from Fig. 3. The curve $G(x, y(x))$ by construction starts from $G(0) = 0$, and increases to values of the order G_{exp}^{∞} when $x \sim s_v$. Obviously, if $s_v \to 0$, this first transition becomes very sharp, and in the limit of $s_v = 0$, this curve may be considered exactly vertical. Thus the intersection of the curves $G(x, y(x))$ and a/β (a horizontal line) corresponds to values $x = 0$ for all β above a threshold. This corresponds to the models with a singular equilibrium considered by Berezovskaya et al. (2007). In this paper, homoclinic orbits originating from, and converging to the origin, have been described and interpreted as extinction in systems of ODEs. Here we recovered this behavior as a singular limiting case of a more general class of frequency-dependent models.

Appendix C. Slow virus spread: the effect of the cancer growth term

C.1. Exponential cancer growth

Let us specify the simplest, exponential, growth law for the cancer cells,

$$F(x, y) = 1.$$

The fixed points of the corresponding system can be found explicitly

$$x_t = 0, \quad x_{0,s} = \frac{1}{2\lambda}(-(a+(1-\beta)\lambda) \mp Q), \quad y_{t,0,s} = \frac{x_{0,i,s}\lambda}{a},$$

where we defined

$$Q \equiv \sqrt{(a+(1-\beta)\lambda)^2 - 4a\lambda}.$$

The subscript t refers to "trivial", and subscripts 0 and s correspond to the internal and saddle equilibria. The non-trivial points are real and positive as long as $\beta > \beta_c$, with $\beta_c = (\sqrt{a}+\sqrt{\lambda})^2/\lambda$. The point x_0 decays with β, and the point x_s grows with β. For large values of β, we have

$$x_0 \sim \frac{a}{\lambda\beta}, \quad x_s \sim \beta.$$

Stability of the internal equilibrium: The eigenvalues corresponding to solution (x_0, y_0) are given by

$$\frac{1}{4\beta\lambda}(P \pm \sqrt{P^2 - 16a\beta\lambda Q}), \quad P = \beta\lambda(1-a) + (a+1)(a-\lambda) - (1-a)Q.$$

The stability of the internal equilibrium is defined by parameters a, λ and β. The sign of the real parts of the eigenvalues corresponds to the sign of P. We will now study the sign of this quantity, as a function of β.

First we note that

$$\frac{\partial P}{\partial \beta} = \frac{2(a-1)\lambda^2 x_0}{Q}.$$

Therefore, P decays for $a < 1$ and grows for $a > 1$. Next let us determine if P changes sign for positive values of β. The equation

$P(\beta)=0$ has a root if

$$1\le a\le\lambda,\quad 1\le 1/\lambda\le a,\quad a\le 1/\lambda\le 1,\quad \lambda\le a\le 1.$$

In these cases we have $P(\beta_0)=0$ with

$$\beta_0=\frac{(a-\lambda)^2}{(a-1)(1-\lambda)\lambda}.$$

We can see that this root is positive only if $a\le 1\le\lambda$ or $\lambda\le 1\le a$. Combining these conditions with the conditions above, we determine that there exists a positive β_0 if

$$1\le 1/\lambda\le a \quad \text{or} \quad a\le 1/\lambda\le 1.$$

Since

$$\beta_0-\beta_c=\frac{(\sqrt{a}(\lambda-1)+\sqrt{\lambda}(a-1))^2}{(1-a)(\lambda-1)\lambda}$$

we can see that $\beta_0>\beta_c$ as long as $\beta_0>0$.

In the cases where P does not change sign, we can determine its sign by looking at the quantity

$$\lim_{\beta\to\infty}P(\beta)=2a(1-\lambda).$$

Combining these results, we obtain a full chart of the signs of P, which corresponds to the stability properties of equilibrium (x_0,y_0). This is presented in Table 2. There are the following special cases: if $\lambda=1$ (the case where $\varepsilon_1=\varepsilon_2$, considered above), we have $\beta_0=\infty$, such that for $a\lambda=a>1$, $P<0$, and for $a\lambda<1$, $P>0$. Also, if $a\lambda=1$, then $\beta_0=\beta_c$, such that for $\lambda>1$, $P<0$ and for $\lambda<1$, $P>0$. Finally, if $\beta=\beta_0$, $P=0$ in all cases.

Note that the results for large values of β, as seen from the table and our calculations, are as follows: for $\lambda>1$, the equilibrium is stable, and for $\lambda<1$ it is unstable. If $\lambda=1$, then it is stable for $a>1$ and unstable for $a<1$. These results can be obtained from our general methods, Eqs. (6) and (11). For the functions F and G discussed here, we have

$$G(x_0,y_0)(m_{11}+m_{22})=\frac{1-\lambda}{\varepsilon_1^2\varepsilon_2}x_0^2+\frac{(\lambda-a)(2-\lambda)}{a\varepsilon_1^3\varepsilon_2}x_0^3,$$

where we used the original, unscaled variables x and y. One can see that for $\lambda\neq 1$, the stability is decided by the quantity $\lambda-1$. For $\lambda=1$, the first term in the expansion disappears, and we use the next term, which is proportional to $1-a$.

Oscillations: To determine if the eigenvalues have an imaginary part, we need to consider the expression

$$W(\beta)=P^2-16a\beta\lambda Q.$$

We have

$$W(\beta_c)=4a(\sqrt{a}(\lambda-1)+\sqrt{\lambda}(a-1))^2>0,$$
$$\lim_{\beta\to\infty}W(\beta)=\lim_{\beta\to\infty}-(4a\lambda^2\beta)^2=-\infty.$$

Therefore, for small values of β the eigenvalues are real and for large values they are complex.

Simulations show that for all λ, there exists one value of β, $\beta_{osc}>\beta_c$, such that for $\beta<\beta_{osc}$ the eigenvalues are real and for $\beta>\beta_{osc}$, the imaginary part becomes non-zero. We have found this value analytically for the special cases of $\varepsilon_1\to\infty$ and $\varepsilon_2\to\infty$. The results are as follows.

If $\lambda\to 0$ ($\varepsilon_2\to\infty$), the quantity $(\beta_{osc}-\beta_c)/\beta_c$ becomes large if $a\to 0$, and it behaves as

$$\frac{\beta_{osc}-\beta_c}{\beta_c}\sim\frac{1}{2\sqrt{a}}.$$

In this case the point (x_0,y_0) is unstable, see Table 2.

If $\lambda\to\infty$ ($\varepsilon_1\to\infty$), the quantity $(\beta_{osc}-\beta_c)/\beta_c$ becomes large if $a\to\infty$, and it behaves as

$$\frac{\beta_{osc}-\beta_c}{\beta_c}\sim\frac{\sqrt{a}}{2}.$$

Eigenvectors and phase portraits: Let us now study the unstable and the stable manifolds of the saddle point (x_s,y_s). Let us first set $\beta=\beta_c$. If $\lambda a>1$, the stable manifold has the eigenvector $(\sqrt{a/\lambda^3},1)^T$, and the unstable one the eigenvector $(a/\lambda,1)^T$. They are reversed if $\lambda a<1$. Note that $\sqrt{a/\lambda^3}<a/\lambda$ if $\lambda a>1$, and the inequality is reversed for $\lambda a<1$, we conclude that the slope of the stable manifold at $\beta=\beta_c$ is larger than that of the unstable one. Numerical simulations suggest that the slope of the stable eigenvector increases with β, and the slope of the unstable one decreases, such that the slope of the stable manifold remains larger than that of the unstable one for all β. Finally, we take the limit of large values of β. We have the stable eigenvector $(0,1)$ and the unstable one $(1,0)$. This means that for large values of β, the stable manifold tends to a vertical line, and the unstable one to a horizontal line.

If $a=1/\lambda$ and $\beta=((1+\lambda)/\lambda)^2$, then both eigenvalues are zero and both eigenvectors are $(\lambda^{-2},1)^T$. This point is the only one where the slopes of the eigenvectors coincide.

In the case where the behavior of the intermediate equilibrium is oscillatory (that is, for large values of β), there are two types of phase portraits, depending on whether the internal equilibrium is stable or unstable. They are presented in Fig. 7, where (a) corresponds to a stable internal equilibrium and (b) to an unstable one.

C.2. Logistic growth

It is interesting to see what happens if we add saturation in the term F. Using the functional form $F(x+y)=1-(x+y)/W$, we have the corresponding term in the rescaled equation $1-(x+y/\lambda)/W$, where $\tilde{W}=W/\varepsilon_1$, and the tilde is omitted. If W is very large, the phase portrait is similar to that of the original, unsaturated equation. The same three equilibria (the trivial point S_t, the internal equilibrium S_0 and the saddle equilibrium S_s) are present, and the difference is that there are two more fixed points in the system. One of them is a saddle $(W,0)$ and the other point, S_c, is a

Table 2
Stability conditions for the equilibrium (x_0,y_0).

	$a\lambda>1$	$a\lambda<1$
$\lambda>1$	$P<0$	$P>0$ for $\beta<\beta_0$, $P<0$ for $\beta>\beta_0$
$\lambda<1$	$P<0$ for $\beta<\beta_0$, $P>0$ for $\beta>\beta_0$	$P>0$

$P>0$ corresponds to the equilibrium being unstable and $P<0$—stable.

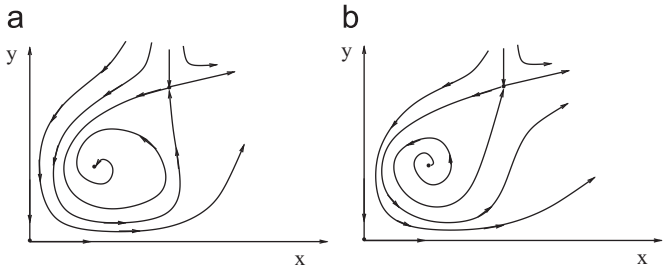

Fig. 7. The phase portrait for system with $F=r$ and $G=x(1+\varepsilon_1)(1+\varepsilon_2)/[(x+\varepsilon_1)(y+\varepsilon_2)]$, a schematic: (a) the intermediate equilibrium is stable and (b) it is unstable.

stable node with a relatively large value of x and a non-trivial y. This latter point is infinitely far when $W \to \infty$; for large values of W it is given by

$$x_c = W - \frac{1+a}{a}\left(\beta - \frac{a}{\lambda}\right), \quad y_c = \frac{\lambda\beta}{a} - 1.$$

As W decreases, the point x_c decreases, and eventually a bifurcation happens which changes the system's behavior. The point S_c collides with the point S_s and they annihilate. There are two separate cases based on the properties of the point S_0:

- If S_0 is a stable spiral, then we have a typical saddle-node bifurcation, resulting in only one, globally stable, fixed point S_0.
- If S_0 is an unstable spiral, the picture is more complicated. As W decreases, first the stable node S_c becomes a stable spiral. Thus we have an unstable and a stable spiral (points S_0 and S_c respectively) separated by a saddle point, S_s. Then, as W decreases even further, the points S_c and S_s collide and annihilate, giving rise to a stable limit cycle around the point S_0.

C.3. Linear growth

Now we use $F(x+y) = r\eta/(x+y+\eta)$. Rescaling $\tilde{\eta} = \eta/\varepsilon_1$, we obtain the growth term:

$$\frac{x\eta}{x+y/\lambda+\eta}.$$

In this case there are exactly four fixed points in the system. We set $\lambda = 1$ to simplify the analysis of the equilibria. One of them is always negative. Another one (S_0) is the usual saddle point, $(0,0)$. The third one corresponds to S_0 for large η and is a spiral. The fourth one corresponds to the saddle point S_s for large values of η. The value x_s, as a function of η, has a discontinuity. As η decreases, it grows and tends to $+\infty$ as $\eta \to \eta_c$ on the right. On the left of that point, $x_s \to -\infty$, and for $\eta < \eta_c$ we have $x_s < 0$.

In order to find the point η_c, we can use the analytical solution for the value x_s obtained as a solution of a cubic equation (because S_0 factors out). The denominator of this expression as a function of η has three zeros, corresponding to

$$\eta = \beta - a, \quad \eta = (q_1 \pm \sqrt{3q_2})/(2a), \tag{25}$$

where $q_1 = \beta - 3(a+1)$ and $q_2 = -\beta^2 - 2(a+1)\beta - (a^2 - 6a - 3)$. We can see that $q_2 < 0$ for $\beta > \beta'$, with $\beta' = -(1+a) + 2\sqrt{1+2a} < \beta_c$, so clearly the second and the third roots in expression (25) are always complex. Therefore, we have

$$\eta_c = \beta - a.$$

To summarize, as η decreases (which in general terms corresponds to a decrease in the cancer scale, s_t), we observe a change in the number of equilibria. This result was obtained and discussed in general terms in previous sections of this paper. The two examples considered here (the logistic and linear growth) illustrate the following point. Depending on the exact growth term, we can have very different types of bifurcation experienced by the system as the viral scale decreases. Each system demonstrates its own unique features. A detailed analysis of each type of terms can be performed. However, we would like to argue that such bottom-up approach is not very fruitful, because it is difficult to generalize on the basis of several particular examples. In our top-down approach, where we analyzed the system before we specified particular functional forms of the cancer and virus terms, we were able to uncover features of behavior common to all realizations of the unknown cancer and virus terms. Particular examples can be studied as more biological information becomes available to further specify the relevant terms in the equations.

References

Adam, J.A., Bellomo, N., 1997. A Survey of Models for Tumor–Immune System Dynamics. Birkhauser, Boston.

Aghi, M., Martuza, R.L., 2005. Oncolytic viral therapies—the clinical experience. Oncogene 24, 7802–7816.

Anderson, R.M., May, R.M., 1991. Infectious Diseases of Humans. Oxford University Press, Oxford, England.

Bajzer, Z., Carr, T., Josic, K., Russell, S.J., Dingli, D., 2008. Modeling of cancer virotherapy with recombinant measles viruses. J. Theor. Biol. 252, 109–122.

Bell, J.C., 2007. Oncolytic viruses: what's next? Curr. Cancer Drug Targets 7, 127–131.

Bell, J.C., Lichty, B., Stojdl, D., 2003. Getting oncolytic virus therapies off the ground. Cancer Cell 4, 7–11.

Berezovskaya, F.S., Novozhilov, A.S., Karev, G.P., 2007. Population models with singular equilibrium. Math. Biosci. 208, 270–299.

Crompton, A.M., Kirn, D.H., 2007. From ONYX-015 to armed vaccinia viruses: the education and evolution of oncolytic virus development. Curr. Cancer Drug Targets 7, 133–139.

Davis, J.J., Fang, B., 2005. Oncolytic virotherapy for cancer treatment: challenges and solutions. J. Gene Med. 7, 1380–1389.

Dingli, D., Cascino, M.D., Josic, K., Russell, S.J., Bajzer, Z., 2006. Mathematical modeling of cancer radiovirotherapy. Math. Biosci. 199, 55–78.

Friedman, A., Tian, J.P., Fulci, G., Chiocca, E.A., Wang, J., 2006. Glioma virotherapy: effects of innate immune suppression and increased viral replication capacity. Cancer Res. 66, 2314–2319.

Harrison, D., Sauthoff, H., Heitner, S., Jagirdar, J., Rom, W.N., Hay, J.G., 2001. Wild-type adenovirus decreases tumor xenograft growth but despite viral persistence complete tumor responses are rarely achieved—deletion of the viral E1b-19-kD gene increases the viral oncolytic effect. Hum. Gene Ther. 12, 1323–1332.

Kaplan, J.M., 2005. Adenovirus-based cancer gene therapy. Curr. Gene Ther. 5, 595–605.

Kelly, E., Russell, S.J., 2007. History of oncolytic viruses: genesis to genetic engineering. Mol. Ther. 15, 651–659.

Kirn, D.H., McCormick, F., 1996. Replicating viruses as selective cancer therapeutics. Mol. Med. Today 2, 519–527.

Lorence, R.M., Pecora, A.L., Major, P.P., Hotte, S.J., Laurie, S.A., Roberts, M.S., Groene, W.S., Bamat, M.K., 2003. Overview of phase I studies of intravenous administration of PV701, an oncolytic virus. Curr. Opin. Mol. Ther. 5, 618–624.

McCallum, H., Barlow, N., Hone, J., 2001. How should pathogen transmission be modelled? Trends Ecol. Evol. 16, 295–300.

McCormick, F., 2003. Cancer-specific viruses and the development of ONYX-015. Cancer Biol. Ther. 2, S157–S160.

McCormick, F., 2005. Future prospects for oncolytic therapy. Oncogene 24, 7817–7819.

Novozhilov, A.S., Berezovskaya, F.S., Koonin, E.V., Karev, G.P., 2006. Mathematical modeling of tumor therapy with oncolytic viruses: regimes with complete tumor elimination within the framework of deterministic models. Biol. Direct 1, 6.

Nowak, M.A., May, R.M., 2000. Virus dynamics, Mathematical Principles of Immunology and Virology. Oxford University Press, Oxford.

O'Shea, C.C., 2005. Viruses—seeking and destroying the tumor program. Oncogene 24, 7640–7655.

Parato, K.A., Senger, D., Forsyth, P.A., Bell, J.C., 2005. Recent progress in the battle between oncolytic viruses and tumours. Nat. Rev. Cancer 5, 965–976.

Post, D.E., Shim, H., Toussaint-Smith, E., Van Meir, E.G., 2005. Cancer scene investigation: how a cold virus became a tumor killer. Future Oncol. 1, 9247–9258.

Roberts, M.S., Lorence, R.M., Groene, W.S., Bamat, M.K., 2006. Naturally oncolytic viruses. Curr. Opin. Mol. Ther. 8, 314–321.

Sigmund, K., 2007. Kolmogorov and population dynamics. In: Charpentier, E., Lesne, A., Nikolski, N.K. (Eds.), Kolmogorov's Heritage in Mathematics. Springer, Berlin, Heidelberg, pp. 177–186.

Vaha-Koskela, M.J., Heikkila, J.E., Hinkkanen, A.E., 2007. Oncolytic viruses in cancer therapy. Cancer Lett 254, 178–216.

Wein, L.M., Wu, J.T., Kirn, D.H., 2003. Validation and analysis of a mathematical model of a replication—competent oncolytic virus for cancer treatment: implications for virus design and delivery. Cancer Res. 63, 1317–1324.

Wodarz, D., 2001. Viruses as antitumor weapons: defining conditions for tumor remission. Cancer Res. 61, 3501–3507.

Wodarz, D., 2003. Gene therapy for killing p53-negative cancer cells: use of replicating versus nonreplicating agents. Hum. Gene Ther. 14, 153–159.

Wodarz, D., Komarova, N.L., 2005. Computational Biology of Cancer. In: Lecture Notes and Mathematical Modeling. World Scientific, Singapore.

Wodarz, D., Komarova, N.L., 2009. Towards predictive computational models of oncolytic virus therapy: basis for experimental validation and model selection. PLoS ONE 4 (1), e4271.